Divergent processing of FVIII light chain variants: secretory potential *versus* proteasomal retention

Heike Singer,[1*] Payal Chawla,[1*] Katrin J. Czogalla-Nitsche,[1] Pujan Engels,[1] Francesco Forin,[1] Marc Sylvester,[2] Melanie Rath,[1] Jens Müller,[1] Tobias Feist,[1] Behnaz Pezeshkpoor,[1] Rawya Al-Rifai,[1] Osman El-Maarri[1] and Johannes Oldenburg[1]

[1]Institute of Experimental Haematology and Transfusion Medicine and [2]Medical Faculty, Core Facility Mass Spectrometry, Institute of Biochemistry and Molecular Biology, University of Bonn, Bonn, Germany

**HS and PC contributed equally as first authors.*

Correspondence: J. Oldenburg
johannes.oldenburg@ukbonn.de

Received: May 15, 2025.
Accepted: November 14, 2025.
Early view: November 27, 2025.

https://doi.org/10.3324/haematol.2025.288250

Supplemental Information

Divergent processing of FVIII light chain variants: secretory potential versus proteasomal retention

Heike Singer,[1,*] Payal Chawla,[1,*] Katrin J. Czogalla-Nitsche,[1] Pujan Engels,[1] Francesco Forin,[1] Marc Sylvester,[2] Melanie Rath,[1] Jens Müller,[1] Tobias Feist,[1] Behnaz Pezeshkpoor,[1] Rawya Al-Rifai,[1] Osman El-Maarri,[1] Johannes Oldenburg,[1,#]

[1]Institute of Experimental Hematology and Transfusion Medicine, University of Bonn, Germany

[2]Medical Faculty, Core Facility Mass Spectrometry, Institute of Biochemistry and Molecular Biology, University of Bonn, Bonn, Germany

#Correspondence: johannes.oldenburg@ukbonn.de

[*]HS and PC contributed equally as co-first authors

EXPERIMENTAL MODEL AND STUDY PARTICIPANT DETAILS

Reprogramming blood from HA-patients

For proof of pluripotency stable iPS cell clones were characterized similarly (Figure S1 & S2). Silencing of the reprogramming transgene was confirmed by endpoint PCR detecting episomal vectors using two sets of primer (oriP and EBNA-1) (Figure S1). Genomic integrity was proven using the microarray PsychArray-24 (Illumina) (Figure S3).

METHOD DETAILS

CRISPR knockout of F8 in iPS wild type

As a negative control for ELISA measurements and immunofluorescent stainings a *F8* iPS knock-out cell line was generated using CRISPR/Cas9 (Figure S4). A custom-made, all-in-one gRNA-Cas9 plasmid with a pRP vector backbone (Vector ID: VB191212-1282zuu) was purchased from VectorBuilder. This vector includes an eGFP sequence to track transfection efficiency, a puromycin resistance cassette for selection, a sequence encoding hCas9 and two gRNAs targeting exon 1 and exon 3 of *F8* (GCCACCAGAAGATACTACCT and TCTGCTAGGTCCTACCATCC). Cm1 wild type iPS cells were transiently transfected with the gRNA-Cas9 plasmid with Lipofectamine Stem Transfection Reagent according to manufacturer's recommendation. 24 hours after transfection cells were selected for two days with 0.3 µg/ml puromycin. After selection, iPS cells were seeded at a concentration of 0.5 cells/well in Matrigel-coated 96-well plates to obtain single cells for clonal expansion. iPS cells were cultured in mTeSR supplemented with 10 µM ROCK inhibitor during transfection, selection and the first three days of clonal expansion. Single cell clones were analyzed by Sanger Sequencing to verify the disruption of *F8* reading frame by INDEL formation following Cas9 DNA cleavage. The following primers were used for both *F8* exon 1 and exon 3 amplification and Sanger Sequencing: *F8* ex1-F (CCCTCCTGGGAGCTAAAGAT), *F8* ex1-R (CACCTTCCTCCAAGCAGACT), *F8* ex3-F (GCTTCTCCACTGTGACCTTGA), *F8* ex3-R (TGACAGGACAATAGGAGGGTATTT).

Differentiation of iPS cells into vascular ECs

Briefly, after generating a single cell suspension of iPS cells, 5,3 x 10^4/cm^2 cells were re-seeded on matrigel in mTeSR1 containing rock inhibitor Y-27632 (final conc 10 µM). Cells were maintained in mesoderm priming medium (MPM) containing DMEM/F12 supplemented with N2 (10 µl/mL), B27 (20 µl/mL), BMP4 (Bone morphogenetic protein-4) (25 ng/mL) and CHIR99021 (Laduviglusib) (8 µM). On day 3, medium was changed. At days 4 to 6, vascular endothelial cell progenitors were induced by maintaining cells in vEC induction medium containing StemPro™-34 supplemented with VEGF-A (200 ng/mL), forskolin (2 µM) and

penicillin/streptomycin (1%). On day 6, cells were detached using Accutase, collected, and centrifuged. Single-cell suspensions were subjected to magnetic activated cell sorting (MACS) for positive selection of CD144 vascular EC (vEC) or CD34 angioblasts according to the manufacturer's instructions.

Differentiation of iPS into iLEC and iLSEC

Day 6 angioblasts for both subtypes were seeded at a cell density of 5,2x10x^4 cells/cm^2 on tissue culture plates coated with fibronectin.

Characterization and functional assays of MACS-isolated vECs

For proof of angiogenic potential, 7x10^4 MACS-isolated vECs were seeded on a 24-well plate coated with 300 µl growth-reduced factor Matrigel^{TM} (Corning) in ECGM-MV2 medium (PromoCell). The ability to form tubular structures was investigated periodically after 2, 4, 6 and 8 hours on a light microscope (Zeiss) (Figures S1C & S2C). For lipid uptake assay, 3x10^4 day 8 vEC's were seeded as biological triplicates in a 96-well plate with ECGM-MV2 medium. After 48 hours medium was supplemented with LDL-DyLight^{TM} 550 (Abcam) (1:100). After 5 hours, degree of LDL uptake was examined under a fluorescent microscope (Axio Observer.7 with ApoTome.2, Zeiss) (Figures. S1C & S2C). Differentiation efficiency between day 0 to 6 was monitored by rt-qPCR (Figure S5).

Specification analysis towards iLEC upon CD144$^+$ MACS separation

For specification analysis marker expression from primary pHUVEC, pHUAEC, pHDLEC and pLSEC was conducted to normalise common, venous, arterial, LEC and LSEC marker to pHUVEC (Figure S6). Starting day 6 CD144+ vECs were cultured in ECGM-MV2 supplemented with low levels of VEGF-A (10 ng/ml). RNAs collected on day 10, 15 and 23 were normalised to pHUAEC for venous marker expression and normalised to HUVEC for arterial and F8 expression (Figure S7). For iLEC specification Trial 1 (T1), vEC were supplemented with VEGF-A (10 ng) and VEGF-C (100 ng) and collected RNAs from day 13, 16 and 21 were analysed for lymphatic marker expression and normalised to pHDLEC. For iLEC specification Trial 2 (T2), vEC were supplemented with VEGF-A (10 ng), VEGF-C (100 ng) and Angiopoietin-1 (20 ng). Collected RNAs from day 10, 16 and 23 were analysed as in T1.

Inflammatory Cytokine Stimulation

Starting day 6 CD144$^+$ vECs were cultured in ECGM-MV2 supplemented with low levels of VEGF-A (10 ng/ml) until day 9. On day 9, the cells were treated with various cytokines for 6 hours (Figure S8). The cytokine treatments included IL-6, IL-3, TNF-α, IL-1β and IFN-γ at concentrations of either 50 ng/ml or 100 ng/ml. Finally in a biological triplicate experiment, cells

were treated with IL-3, TNF-α or IL-6 at concentrations of 20 ng/ml or 50 ng/ml. In control treatments, medium only supplemented with bovine serum albumin (BSA) at concentrations corresponding to those used in cytokine dilutions was added to the cells.

RNA analyses

Total RNA from day 6 $CD144^+$ vEC was isolated using the PureLink™ RNA mini kit, according to the manufacturer's instructions. The concentration and purity of RNA was determined using a ND-1000 spectrophotometer (Nanodrop). cDNA was synthesized using the QuantiNova™ Reverse Transcription Kit. Overlapping rt-PCR was performed according to the published protocol. [59] For specification analyses of the iLEC and iLSEC model, cells were harvested between day 12 to 16 and RNA extractions were prepared using the PureLink™ RNA mini kit, according to the manufacturer's instructions. RT-qPCR for iPS, mesoderm, common EC, venous, arterial, lymphatic and LSEC marker was implemented using the AgPath-ID™-Kit with appropriate primer-probe pair (Table S1).

Following cytokine treatment, day 10 $CD144^+$ vEC were isolated as above and subjected to rt-PCR analysis.

ELISA

GMA012: Plates were coated with the antibody (5 µg/ml) over night. After washing thrice (1x PBS, 0.05% Tween, 3 mM $MgCl_2$) and blocking for two hours with 2% BSA, triplicates from each sample (1:6 dilution) was incubated for four hours at room temperature. Next, wells were washed thrice and further incubated with detection antibody SAF8C-HRP (2 µg/ml). Finally, upon washing, chemiluminescence ELISA substrate was added and luminescence was measured by multi-detection microplate reader (Synergy2, Biotek). Standard curve was prepared using HEK *F8*$^{-/-}$ cellular lysate diluted in NP40 lysis buffer (1:6) adding different concentrations (5, 7.5, 10, 20, 40, 80, 160, 320 mU) of recombinant full-length FVIII (Kogenate). EC specific lysates from Cm1 and I22I were defined as positive controls, whereas EC lysates LDA2 and Cm1 *F8*$^{-/-}$ were used as negative controls.

CaptureSelect™ biotin anti-FVIII conjugate: Wells were coated with streptavidin (1 µg/mL) and incubated overnight. The following day, the plate was washed with washing buffer (1x PBS, 0,05% Tween, 0,1% BSA). Wells were coated with the antibody (2 µg/mL) and incubated for 2 hours at RT. After another washing step, samples were added at a 1:12 dilution with 1xPBS supplemented with 0,1% Tween and 0,1% BSA and incubated for 2 hours at RT. Detection antibody SAF8C-HRP (2 µg/mL) was added and incubated for 1 hour at room temperature post another washing step. After a final wash, the chemiluminescent ELISA substrate was added, and luminescence was measured in the microplate reader using the above-mentioned standard curve (1:12).

FACS analyses

Cells on day 0, 4, 6, 10, 12 and 14 were detached using Accutase collected, centrifuged and stained with primary antibodies according to the manufacturer's instructions 10 minutes at 4°C in FACS buffer (PBS+0.2 mM EDTA+0.5% BSA). Upon incubation, cells were washed and resuspended in FACS buffer for analysis using Beckman Coulter Life sciences, Navios EX flow cytometry platform. Data analysis was further conducted on FlowJo v10.9. Gating based on FMO controls (Figure S9). To evaluate the inflammatory responsiveness and antigen-presenting potential of the differentiated endothelial cells, iPSC-derived vascular endothelial cells (vEC) were stimulated at day 13 of differentiation with 50 ng/ml or 100 ng/ml IFN-γ for 6 h or 24 h (S10-A). Total RNA was isolated and analysed by real-time PCR for *PD-L1* and *PD-L2* expression. In parallel, primary HUVEC, primary HDLEC and iPSC-derived vEC (A10D) were treated with 100 ng/ml IFN-γ for 24 h to determine *CIITA* induction as a transcriptional activator of MHC-II (S10-B). For flow cytometry, iPSC-derived vEC (A10D) and iLSEC (LI-4D E/S) were stimulated with 100 ng/ml IFN-γ for 24 h and stained for MHC-I using REA230 (HLA-A, B, C) and MHC-II using antibody WR18 (HLA-DR, -DQ, -DP). Both endothelial subtypes showed a clear upregulation of MHC-I, while MHC-II was also increased with slightly lower intensity in iLSEC (S10-C).

Immunofluorescence (IF)

Differentiated iLSECs were cultured on 12-well cover slips until day 14. After fixation with 4% paraformaldehyde (RT/10 minutes), cells were blocked with PBS containing 0.1 M Glycine, 1% BSA and 0,1% Saponin for 1 hour at RT. Cells were incubated at 4°C overnight with primary antibodies diluted in PBS containing 1% BSA and 0,1% saponin. Cells were washed with the blocking medium and incubated at RT for 60 minutes with the corresponding secondary antibodies (Table S1).

When stained with biotin anti-FVIII conjugate, cells were additionally blocked with Ready Probes™ Streptavidin/Biotin blocking solution according to the manufacturer´s instructions to avoid cross-reaction with endogenous biotin. Finally, cells were incubated overnight with biotin anti-FVIII conjugate and visualized with Streptavidin Alexa488.

Western Blot

For a second approach, lysates from $10x10^6$ iLSEC were subjected to immunoprecipitation using the monoclonal anti-A2 antibody GMA012. The eluates were then split: one half was directly loaded onto SDS-PAGE and probed by Western blot using SAF8C-AP; the other half underwent PNGase F treatment (New England Biolabs, #P0704S) to assess glycosylation status. Briefly, eluates were denatured in glycoprotein denaturation buffer (10 min, 99 °C), then incubated with PNGase F (1 h, 37 °C) in the presence of GlycoBuffer 2 and NP-40. Following

digestion, samples were mixed with Laemmli buffer (1:1 with BME), heated at 95 °C for 5 min, and loaded on 7,5% TGX gel.

Chromatography parameters and mass spectrometry conditions

Peptide separation was performed on a Dionex Ultimate 3000 RSLC nano HPLC system coupled to an Orbitrap Fusion Lumos mass spectrometer. Dried peptides were dissolved in 10 µl 0.1% formic acid (solvent A) and 15% were injected onto a C18 analytical column (400 mm x100 µm, 3 µm). For targeted analysis, peptides were separated as above (90 min gradient). 24 Coagulation factor VIII peptides across all processed regions were chosen based on the unique SRM peptides in the nextprot database (www.nextprot.org) and manual curation. Precursors with z=2 and / or z=3 were chosen for isolation and fragmentation. MS1 spectra were acquired from 330 to 1200 m/z in the Orbitrap every 3 seconds with a maximum inject time of 50ms (R=60,000, gain control target 400,000). Target ions were subjected to stepped-HCD fragmentation (1.0 Da quadrupole isolation, collision energy 28%) and product ions analysed in the Orbitrap with a maximum inject time of 32 ms (R=15,000, gain control=50,000).

Data analysis

Peptide identification was done with an in-house Mascot server version 2.8.1 against human sequences of SwissProt (2022_02, 20,387 human sequences) and a collection of common contaminants. Precursor ion *m/z* tolerance was 10 ppm, fragment ion tolerance 20 ppm. Tryptic peptides were searched for up to two missed cleavages. Propionamide was set as a static modification of cysteines, while oxidation of methionine and acetylation of protein N-termini were set as dynamic modifications. Spectrum confidence of Mascot results was assessed by the Percolator algorithm 3.05 as implemented in Proteome Discoverer software 2.5.0.400.[60] Spectra without high confident matches (q-value > 0.01) were sent to a second round Mascot search with semi-specific enzyme cleavage and changing the modification of cysteines with propionamide to dynamic. Database search results were maintained at a 1% false discovery rate for reliable protein identifications. Validation of MS2 spectra was aided by a spectral library created on the PROSIT server.[62] Quantification was done on MS2 level.

Quantification and Statistical Analysis

Graph Pad Prism was used to plot heatmap an rt-PCR results. *t*-test was performed between two analyses with $p<0.05$ deemed significant.

IEDB Analysis of MHC-I and MHC-II Binding and Processing

HLA class I (A, B, C) and class II (HLA-DR, DP, DQ) genotyping of the patients was performed using the AllType™ FASTplex™ NGS Assay kits (One Lambda, A Thermo Fisher Scientific)

according to the manufacturer's instructions. DNA sequencing library was sequenced on a MiniSeq DNA sequencer (Illumina Inc., SanDiego, CA). Data analysis was performed using the TypeStream Visual software (One Lambda).

In silico predictions of FVIII-derived peptide presentation were performed using the Immune Epitope Database (IEDB). FVIII wild-type and patient-specific truncated sequences were analyzed. I22I in silico transcript ends after exon 22 (at AA 2143), followed by translation into intron 22 until the first stop codon appears. This yields a truncated peptide ending with three extra amino acids: V, C, N (from GTA, TGT, AAT).

For MHC-I, NetMHCpan 4.1 (EL and BA models) together with the IEDB processing module (proteasome cleavage, TAP transport, binding) and the immunogenicity tool were applied. For MHC-II, NetMHCIIpan 4.1 EL, the CD4 Epitope Score, and the MHC-II NP module were used. Predictions were filtered for strong binders and peptides with high predicted immunogenicity, and results were reported as exploratory analyses (Figures S13–14).

Figures: Created in BioRender. Singh, S. (2025) https://BioRender.com/undefined

Supplemental Figures and Tables:

Figure S1: Functional characterization of iPS and A10D vEC for wild type Cm1 and two HA patient samples I22I and LDA2.

A. Stable iPS cells were characterized by staining with specific pluripotency marker AP Live, Nanog, SSEA-4, Tra-1-60, and Oct-4. B. iPS cell derived embryoid bodies tested for spontaneous differentiation into all three germ layers by immunofluorescent staining (IF) using antibodies against actin smooth muscle (ASM), ß-Tubulin III and α-feto protein. C. Tube forming assay presents the angiogenic potential of CD144 MACS isolated vEC maintained 10 Days in 10ng VEGF-A = A10D (left picture cluster). LDL-uptake assay visualized uptake of LDL-DyLight™ 550 (red signal) in all three samples. D. Transgene silencing was confirmed by PCR specific to episomal vectors. E. Mycoplasma negative PCR in all iPS cell derived patient samples. Immunostaining results depicted as a representative image of biological duplicates.

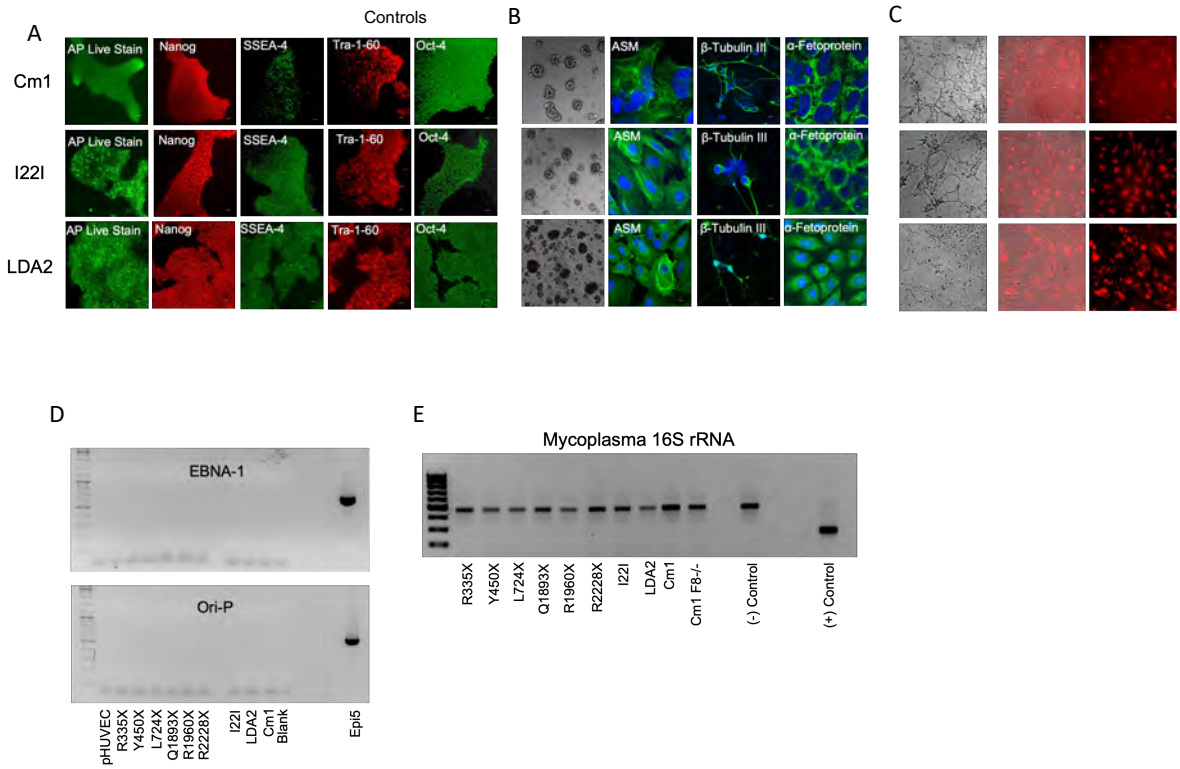

Figure S2: Functional characterization of iPS and A10D vEC for six patient samples with nonsense mutations in the heavy and light chain of FVIII. A. Stable iPS cells were characterized by staining with specific pluripotency marker AP Live, Nanog, SSEA-4, Tra-1-60, and Oct-4.

B. iPS cell derived embryoid bodies tested for spontaneous differentiation into all three germ layers by immunofluorescent staining (IF) using antibodies against actin smooth muscle, β-Tubulin III and alpha-feto protein. C. Tube forming assay presents the angiogenic potential of A10D vEC (left picture cluster). LDL-uptake assay visualized uptake of LDL-DyLight™ 550 (red signal) in all six samples. Immunostaining results depicted as a representative image of biological duplicates.

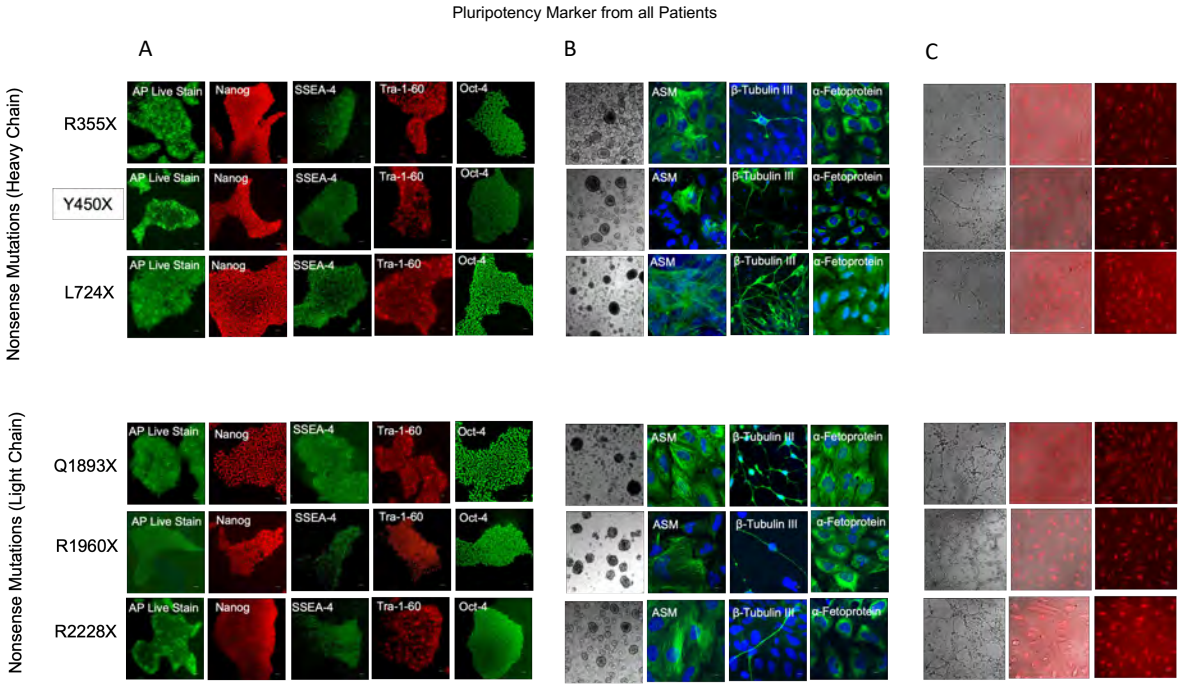

Figure S3: Karyotype analysis.

DNA of stable iPS cell clones from healthy and patients with mutations was analysed using a SNP (single nucleotide polymorphism) array. For each chromosome the B allele frequency (upper blue dotted row) and the log A ratio (lower blue dotted line) was evaluated.

A. Controls: Cm1, Cm1 *F8-/-*, I22I and LDA2

B. Nonsense mutations in the heavy chain: R355X, Y450X, L724X.

C. Nonsense mutations in the light chain: Q1893X, R1960X, R2228X

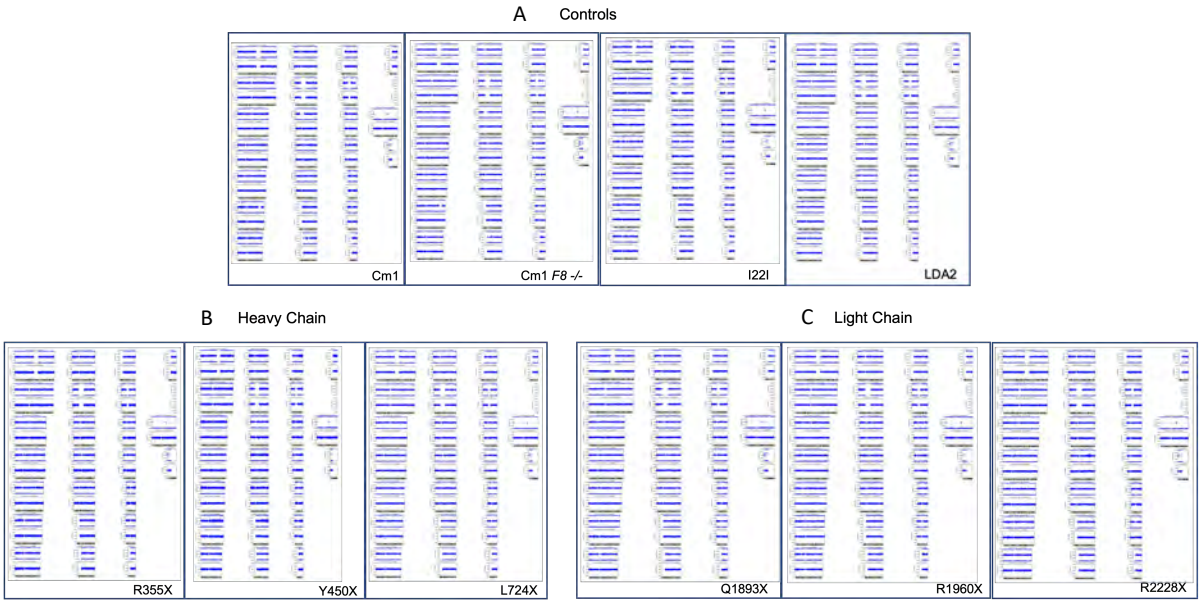

Figure S4: CRISPR-Cas9 mediated knock-out of *F8* gene by targeting exons 1 and 3. The vector map on the left displays two guide RNAs (gRNAs) aimed to target ex1 (green) and ex3 (pink). On the right, sequencing results for IPS clone #31 confirm successful gene disruption. The gRNAs induced a one base pair deletion in exons 1 and 3, causing a frameshift and introducing several premature stop codons.

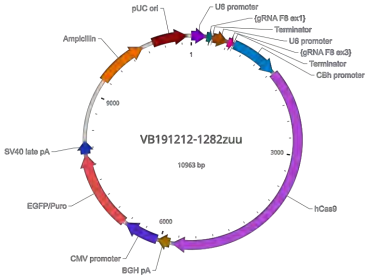

CRISPR vector targeting Ex1&3

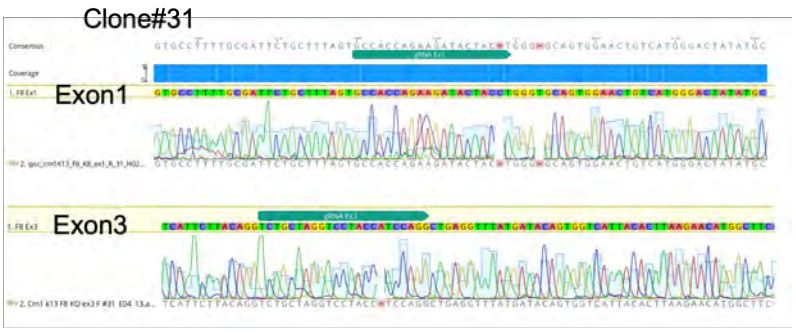

Figure S5: Differentiation efficiency monitored by relative gene expression. On day 0, pluripotency markers *Nanog* and *Sox2* (orange bars) show the highest expression when normalized to β-actin. On day 4, mesodermal marker *Brachyury* (olive bars) shows the highest expression when normalized to β-actin. On day 6, after CD144 MACS isolation endothelial cell marker *CD31* and *CD34* show exclusive expression when normalized to β-actin (light green bars).

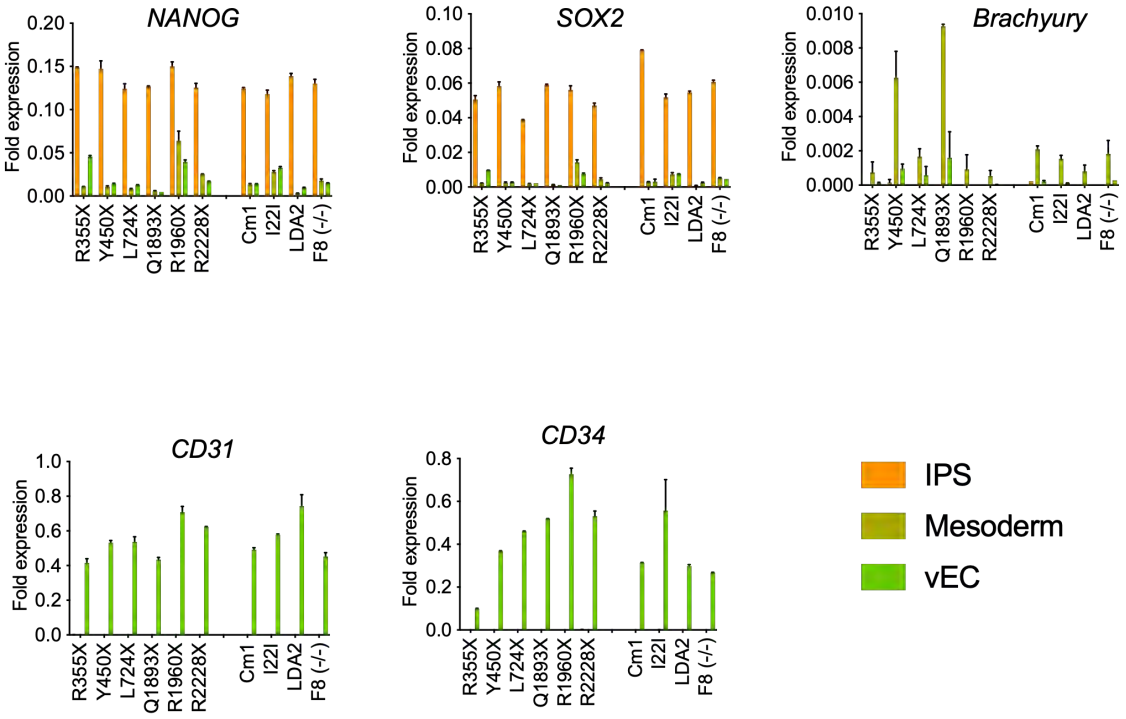

Figure S6: rt-PCR studies for specification of primary human cell lines.

Controls: HUVEC: human umbilical vein endothelial cell, HUAEC: human umbilical arterial endothelial cell, HDLEC: human dermal lymphatic endothelial cell, LSEC: liver sinusoidal endothelial cell. Result denoted as a fold expression to pHUVEC.

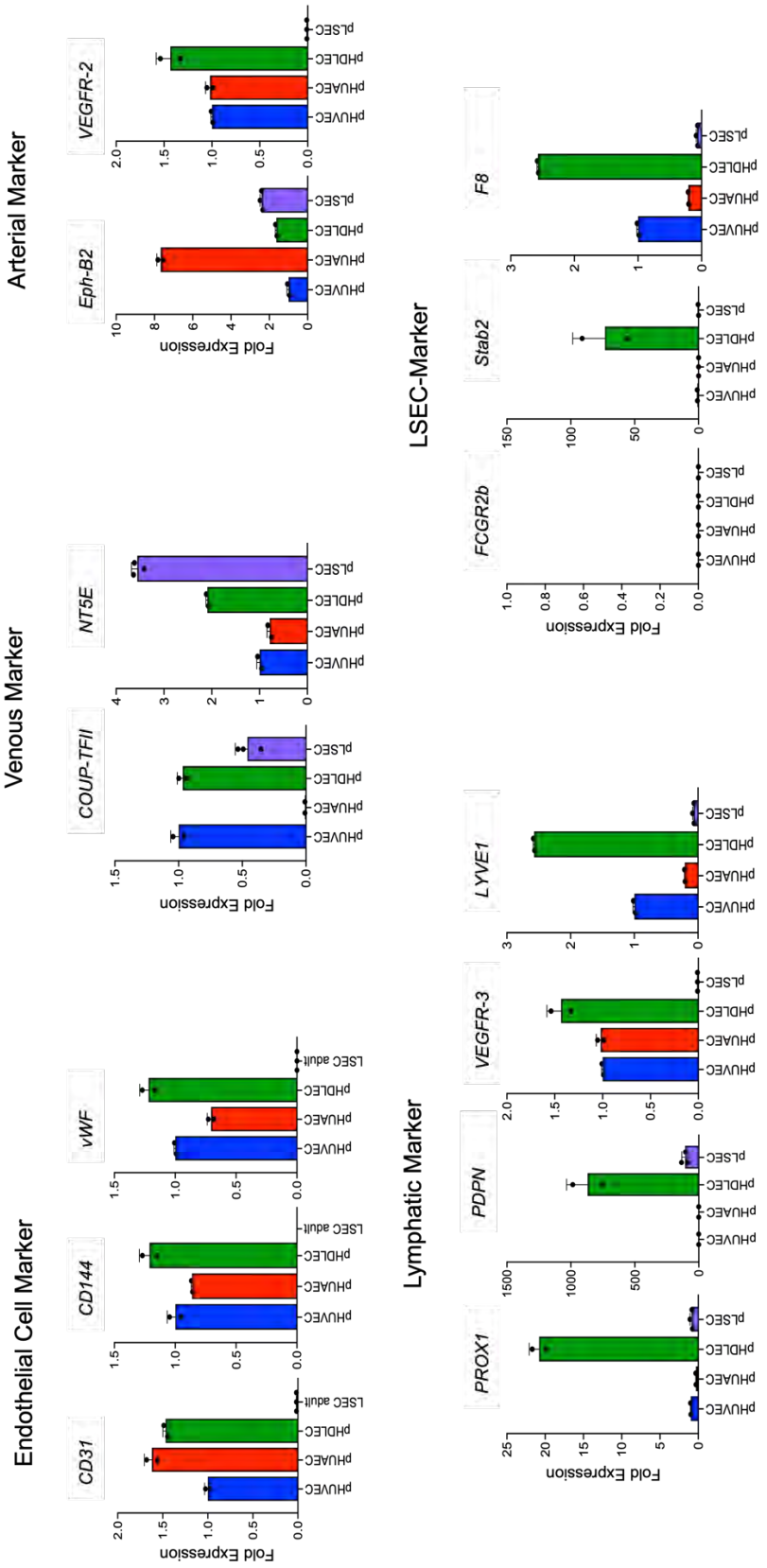

Figure S7: Specification analysis towards iLEC upon CD144^{+} MACS selection.

A. 10 ng VEGF-A: Venous endothelial progenitors were maintained in 10 ng VEGF-A starting day 6. RNA was collected on day 10, 15 and 23.

B. T1: Venous endothelial progenitors were maintained in a combination of 10 ng VEGF-A and 100 ng VEGF-C. RNA was collected on day 13, 16 and 21.

C. T2: Venous endothelial progenitors were maintained in a combination of 10 ng VEGF-A, 50 ng VEGF-C and 20 ng Angiopoietin-1. RNA was collected on day 10,16 and 23.

Controls: HUVEC: human umbilical vein endothelial cell, HUAEC: human umbilical arterial endothelial cell, HDLEC: human dermal lymphatic endothelial cell, HCMEC: human cardiac microvascular endothelial cell. Result denoted as a fold expression to pHUAEC for venous marker, pHUVEC for arterial marker and *F8,* pHDLEC for lymphatic marker.

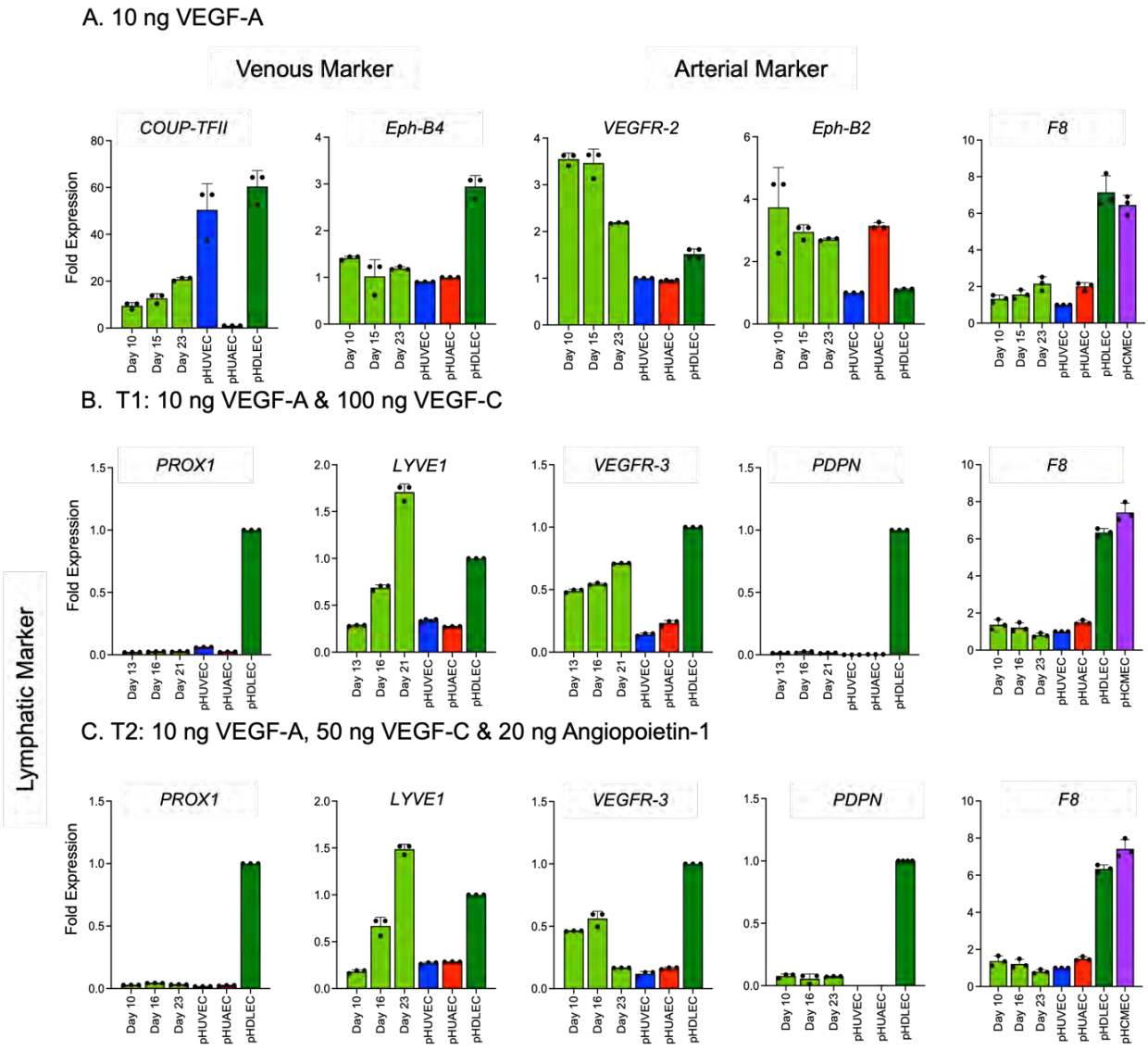

Figure S8: rt-PCR studies to determine inflammatory cytokine influence in vECs and their impact on *F8*.

Cells were treated with 50 ng or 100 ng concentrations of IL-6, IL-3, TNFα, IL-1β and IFN-ɣ for 6 hours and collected as RNA. Grey bars denote untreated cells as control. ***:p<0.001, ****:p<0.0001. Result denoted as fold expression to untreated cells.

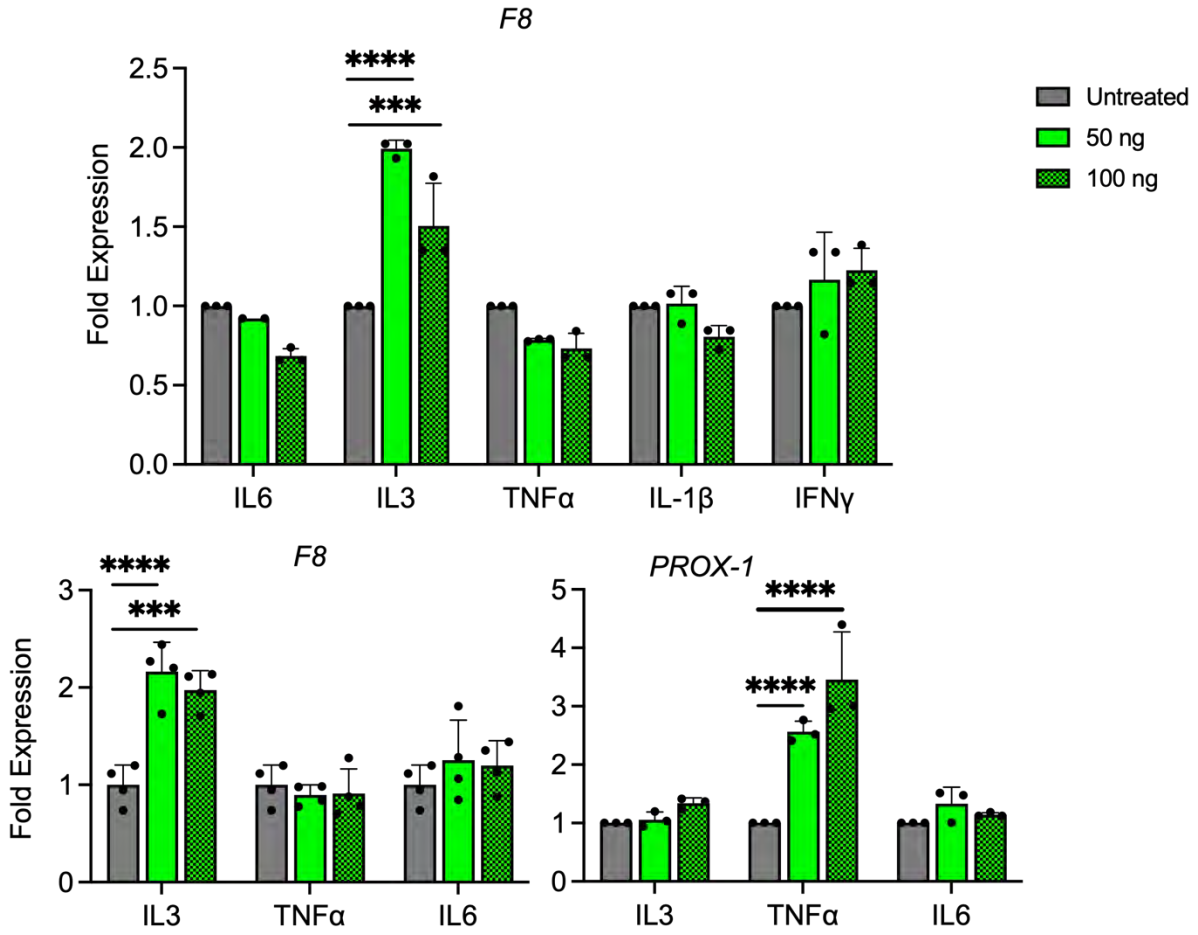

Figure S9: Gating strategy for FACS analysis based on FMO controls. A. A cells gate is created based on FS-A vs SS-A. B. Doublets are removed with a FS-A vs FS-W gate (single cell gate). C. Live cells are selected using a PI as a marker. D. Based on the FMO control of CD34, selection of the CD34+ population was made. E. Similarly using FMO control for CD73 and CD184, selection of a subset of CD34+ cells and subsequent arterial and venous population was selected.

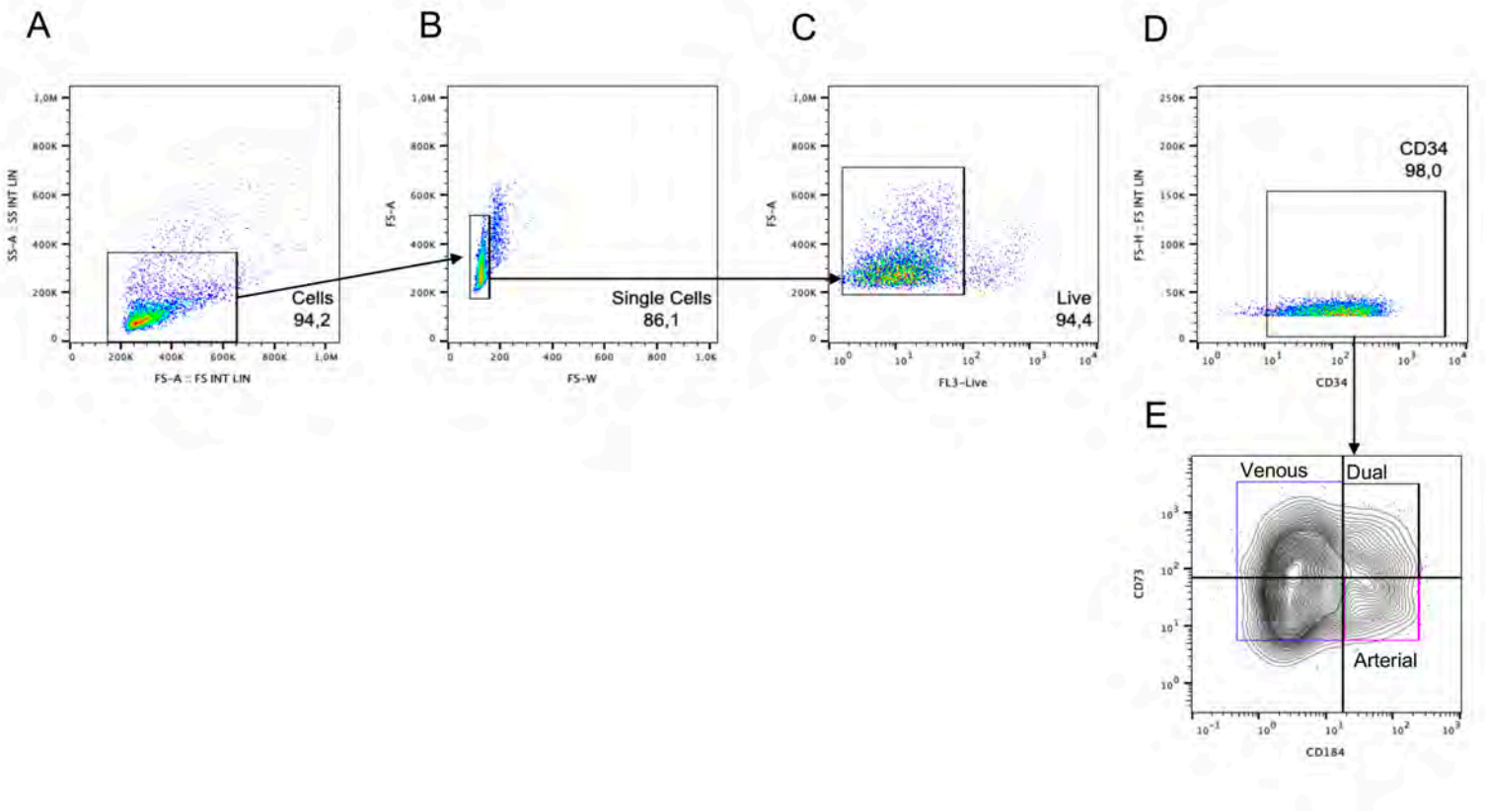

Figure S10. IFNγ–induced immune activation in iPS differentiated endothelial cells.

qPCR and flow cytometry analyses showing induction of *PD-L1*, *PD-L2* and *CIITA* expression as well as upregulation of MHC-I and MHC-II surface molecules in iPSC-derived endothelial cells after IFN-γ stimulation of vEC (A10D) and iLSEC (LI-4D E/S).

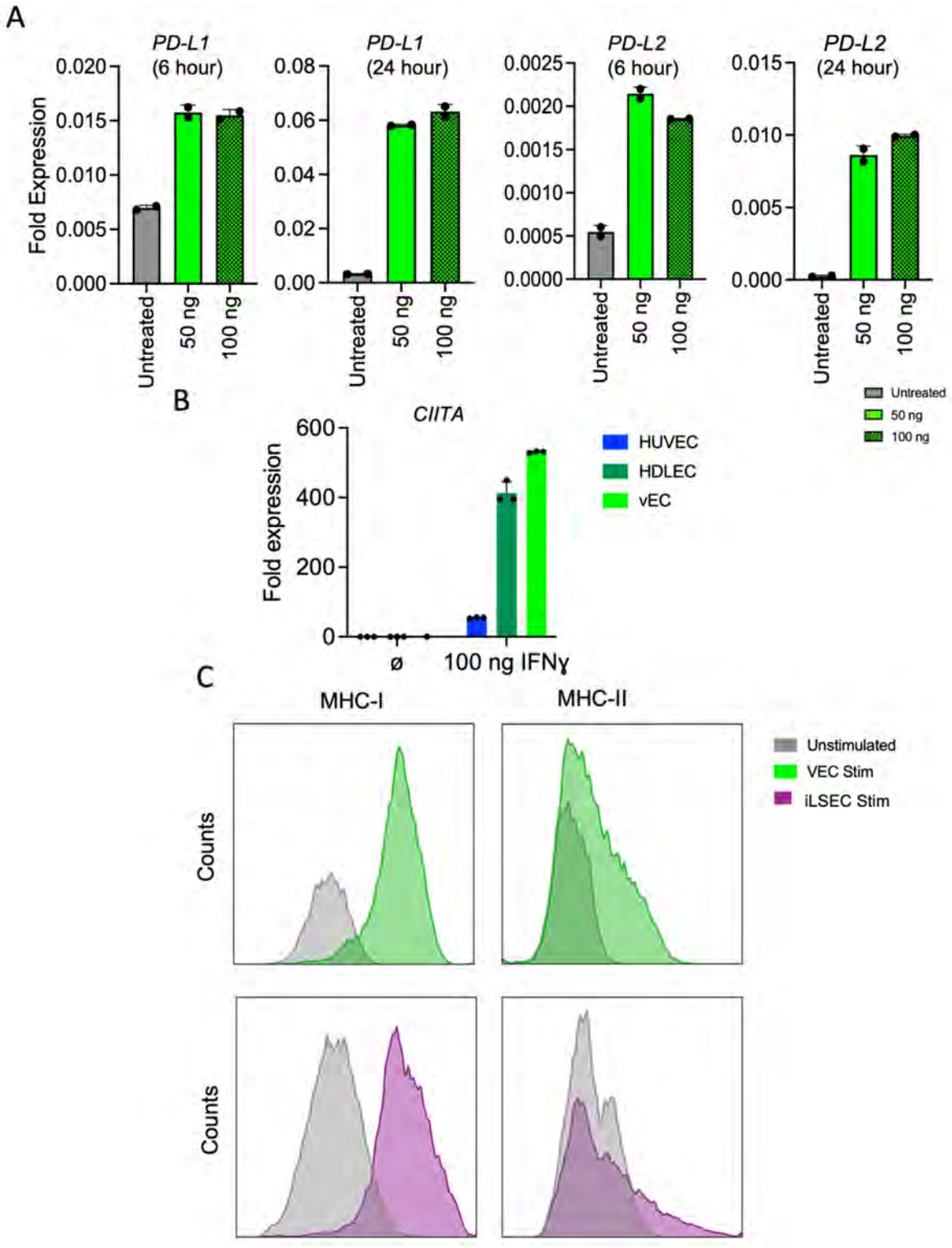

Figure S11: Overlapping semiquantitative rt-PCR representing molecular *F8* mRNA content from vEC differentiated HA-patients (first lane) compared to wild type donor Cm1 (second lane).

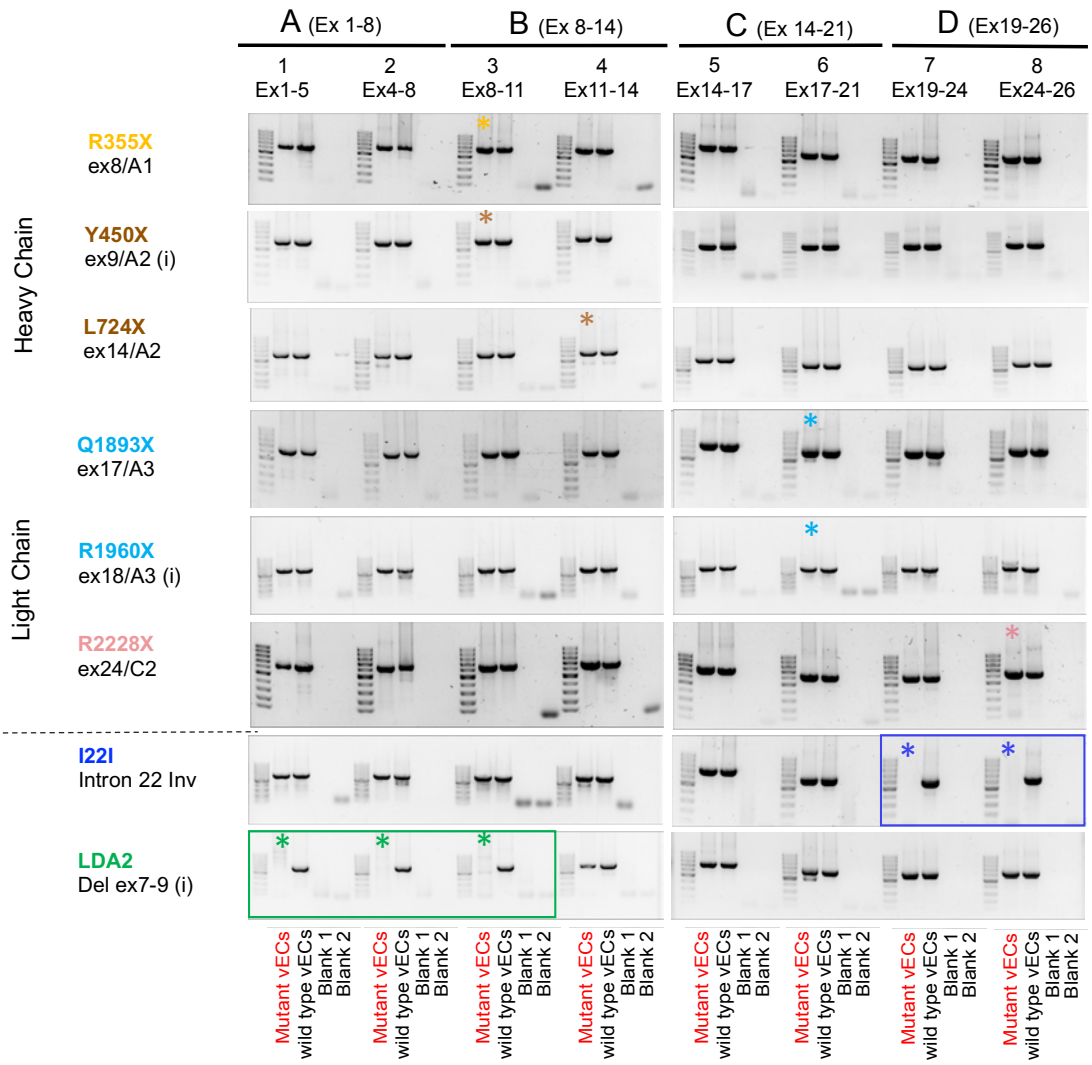

Figure S12: A. Immunostaining with anti-vWF (red) in iPS derived LEC (iLEC) , LSEC (iLSEC) iLSEC Cm1: wild type, pHDLEC: human dermal lymphatic endothelial cell, pHUVEC: human umbilical vein endothelial cell. Nuclei were counterstained with DAPi. Images were acquired using an Axio Observe 7 microscope with ApoTome.2. The objective used was a Plan-Apochromat 40x/1.4 Oil DIC M27. Images were captured with an AxioCam 702 Mono camera.

B. rt-PCR analysis of cell specific markers in vEC and iLSEC using *vWF*. LI-2D E/S: 2 days LI, 1:1 ECGM-MV2 & StemPro-34, LI-4D E/S: 4 days LI, 1:1 ECGM-MV2 & StemPro-34, LI-6D E: 6 days LI, only ECGM-MV2. E/S medium conditions consist of bFGF. Cells cultured in medium condition E does not contain bFGF, A10D: from generic vEC protocol, adding 10 days VEGF-A (Day 6-10). pHUVEC: human umbilical vein endothelial cell, pHUAEC: human umbilical arterial endothelial cell, pHDLEC: human dermal lymphatic endothelial cell, pLSEC: liver sinusoidal endothelial cell. n=200,000 cells. All data points indicate mechanical duplicates.

C. Immunostaining with biotin anti-FVIII conjugate targeting the A3 domain of FVIII visualized with Streptavidin488 (green) in primary HDLEC and anti-vWF(red). Nuclei were counterstained with DAPi. Images were acquired using an Axio Observer 7 microscope with ApoTome.2. The objective used was a Plan-Apochromat 40x/1.4 Oil DIC M27. Images were captured with an AxioCam 702 Mono camera.

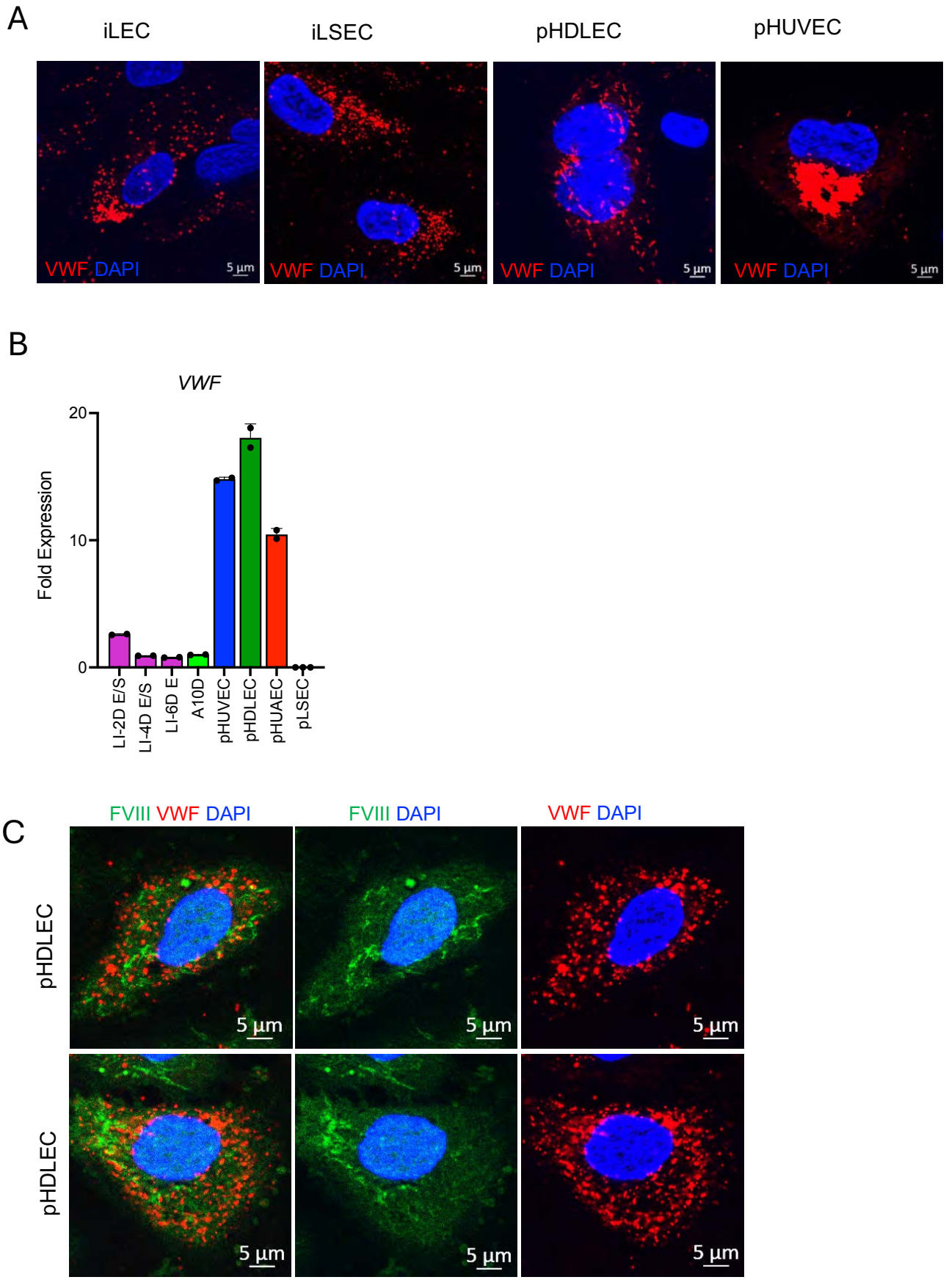
A
iLEC
iLSEC
pHDLEC
pHUVEC
VWF DAPI
5 µm
B
VWF
Fold Expression
20
10
0
LI-2D E/S
LI-4D E/S
LI-6D E
A10D
pHUVEC
pHDLEC
pHUAEC
pLSEC
C
FVIII VWF DAPI
FVIII DAPI
VWF DAPI
pHDLEC
pHDLEC
5 µm

S13: Supplementary Figure 13. MHCI peptide presentation analysis.

(A) Total number of FVIII-derived peptides identified for HLA-A, HLA-B, and HLA-C alleles.

(B) Distribution of FVIII peptides across individual HLA alleles.

(C) Predicted immunogenicity scores of peptides restricted to HLA-A, B, and C, with HLA-B showing significantly higher values. Unpaired t-test significance: ****:p<0.0001.

(D) Immunogenicity of peptides stratified by FVIII domains (A1, A2, A3, C1, C2). Representative peptide sequences, positions, domains, and scores are listed on the right. Bar graphs (far right) depict the proportion of top 10 peptides assigned to FVIII domains across the three patients (R1960X, R2228X, I22I). One-way ANOVA significance:**:p<0.01, ***:p<0.001, ****:p<0.0001.

(E) Processing score (PS) of peptides by FVIII domains. Corresponding sequences with PS values are shown on the right. Bar graphs (far right) show distribution of top 10 peptides by FVIII domains across the three patients.

(F) Predicted peptide loss associated with patient mutations. Venn diagram depicting in silico–predicted FVIII peptides absent due to the premature stop codons R1960X, R2228X, or I22I, with representative sequences.

(G) Venn diagram depicting overlap of high-immunogenic peptides among HLA-A, B, and C alleles. Shared and unique peptides are listed below.

(H) Heatmap of peptide presentation strength across HLA-A, B, and C alleles aligned to patient mutations. Right panel: Venn diagrams depicting allele-specific overlap of presented peptides across three patients.

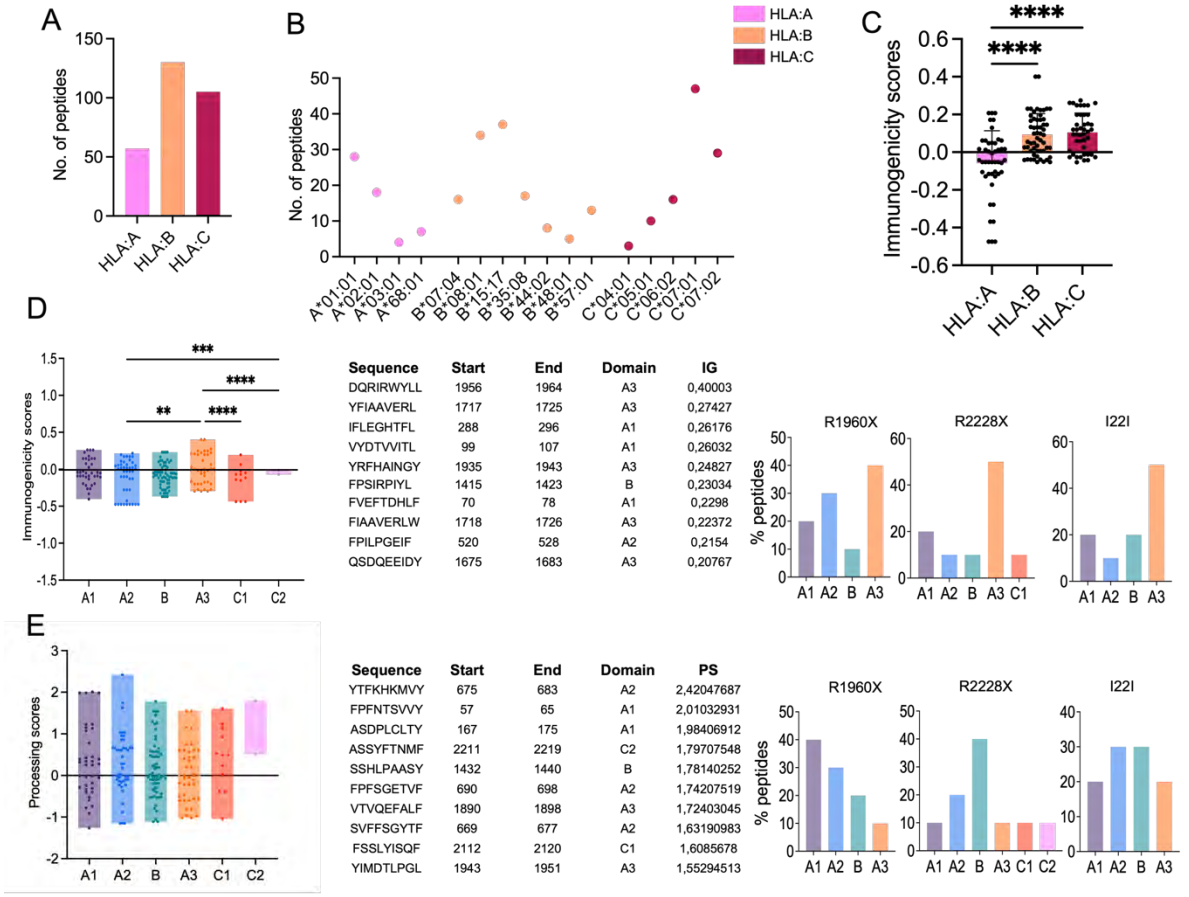
A
No. of peptides
HLA:A
HLA:B
HLA:C
B
HLA:A
HLA:B
HLA:C
No. of peptides
A*01:01
A*02:01
A*03:01
A*68:01
B*07:04
B*08:01
B*15:17
B*35:08
B*44:02
B*48:01
B*57:01
C*04:01
C*05:01
C*06:02
C*07:01
C*07:02
C
Immunogenicity scores
HLA:A
HLA:B
HLA:C
D
Immunogenicity scores
A1 A2 B A3 C1 C2
Sequence Start End Domain IG
DQRIRWYLL 1956 1964 A3 0,40003
YFIAAVERL 1717 1725 A3 0,27427
IFLEGHTFL 288 296 A1 0,26176
VYDTVVITL 99 107 A1 0,26032
YRFHAINGY 1935 1943 A3 0,24827
FPSIRPIYL 1415 1423 B 0,23034
FVEFTDHLF 70 78 A1 0,2298
FIAAVERLW 1718 1726 A3 0,22372
FPILPGEIF 520 528 A2 0,2154
QSDQEEIDY 1675 1683 A3 0,20767
R1960X
R2228X
I22I
% peptides
E
Processing scores
A1 A2 B A3 C1 C2
Sequence Start End Domain PS
YTFKHKMVY 675 683 A2 2,42047687
FPFNTSVVY 57 65 A1 2,01032931
ASDPLCLTY 167 175 A1 1,98406912
ASSYFTNMF 2211 2219 C2 1,79707548
SSHLPAASY 1432 1440 B 1,78140252
FPFSGETVF 690 698 A2 1,74207519
VTVQEFALF 1890 1898 A3 1,72403045
SVFFSGYTF 669 677 A2 1,63190983
FSSLYISQF 2112 2120 C1 1,6085678
YIMDTLPGL 1943 1951 A3 1,55294513
R1960X
R2228X
I22I
% peptides

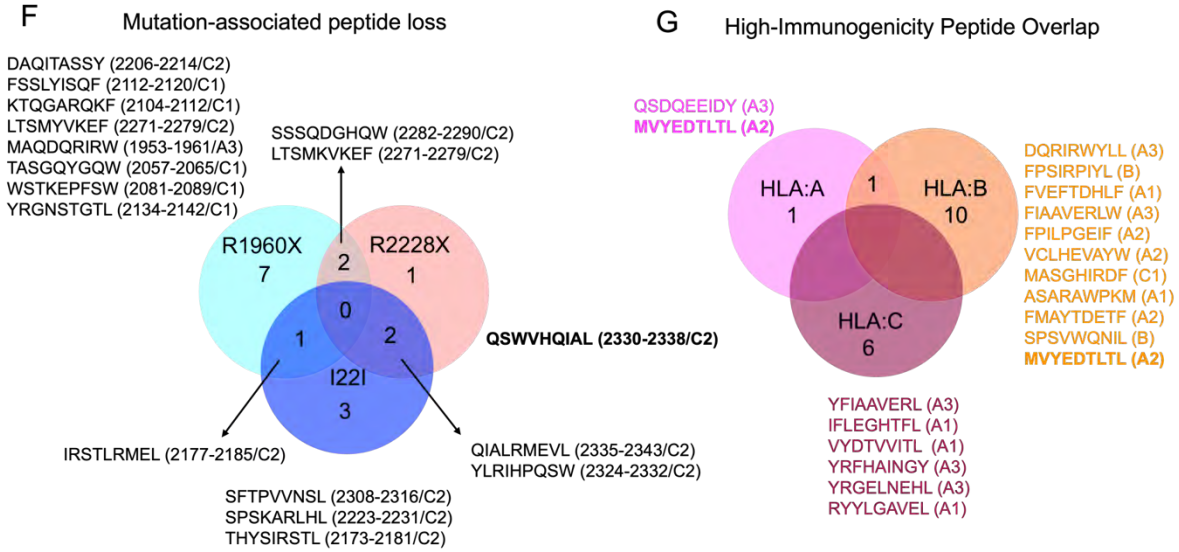
F
Mutation-associated peptide loss
DAQITASSY (2206-2214/C2)
FSSLYISQF (2112-2120/C1)
KTQGARQKF (2104-2112/C1)
LTSMYVKEF (2271-2279/C2)
MAQDQRIRW (1953-1961/A3)
TASGQYGQW (2057-2065/C1)
WSTKEPFSW (2081-2089/C1)
YRGNSTGTL (2134-2142/C1)
SSSQDGHQW (2282-2290/C2)
LTSMKVKEF (2271-2279/C2)
R1960X
7
R2228X
1
I22I
3
2
0
1
2
QSWVHQIAL (2330-2338/C2)
IRSTLRMEL (2177-2185/C2)
QIALRMEVL (2335-2343/C2)
YLRIHPQSW (2324-2332/C2)
SFTPVVNSL (2308-2316/C2)
SPSKARLHL (2223-2231/C2)
THYSIRSTL (2173-2181/C2)
G
High-Immunogenicity Peptide Overlap
QSDQEEIDY (A3)
MVYEDTLTL (A2)
HLA:A
1
HLA:B
10
HLA:C
6
1
DQRIRWYLL (A3)
FPSIRPIYL (B)
FVEFTDHLF (A1)
FIAAVERLW (A3)
FPILPGEIF (A2)
VCLHEVAYW (A2)
MASGHIRDF (C1)
ASARAWPKM (A1)
FMAYTDETF (A2)
SPSVWQNIL (B)
MVYEDTLTL (A2)
YFIAAVERL (A3)
IFLEGHTFL (A1)
VYDTVVITL (A1)
YRFHAINGY (A3)
YRGELNEHL (A3)
RYYLGAVEL (A1)

H

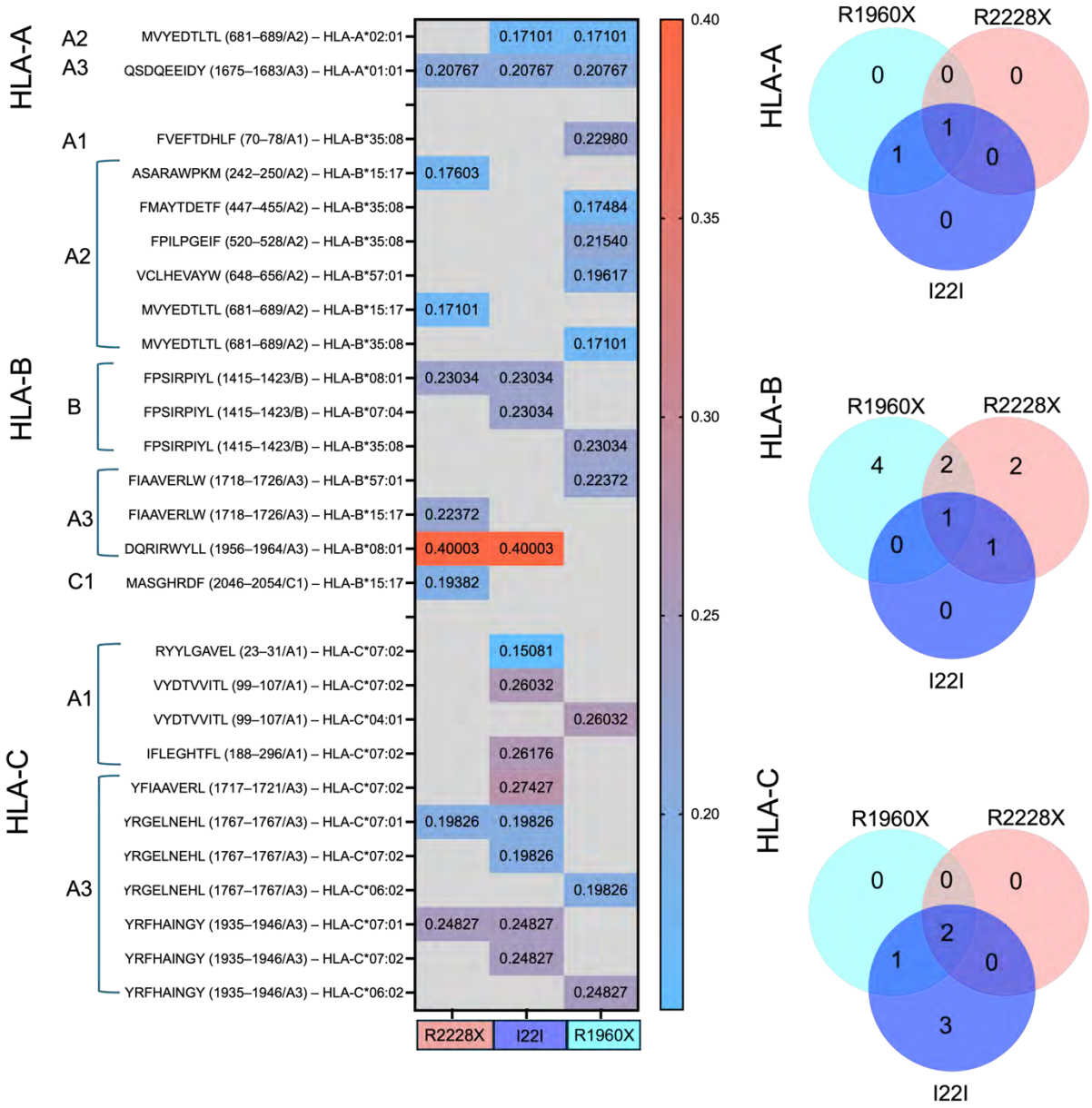
HLA-A
HLA-B
HLA-C
A2
A3
A1
A2
B
A3
C1
A1
A3
MVYEDTLTL (681–689/A2) – HLA-A*02:01
QSDQEEIDY (1675–1683/A3) – HLA-A*01:01
FVEFTDHLF (70–78/A1) – HLA-B*35:08
ASARAWPKM (242–250/A2) – HLA-B*15:17
FMAYTDETF (447–455/A2) – HLA-B*35:08
FPILPGEIF (520–528/A2) – HLA-B*35:08
VCLHEVAYW (648–656/A2) – HLA-B*57:01
MVYEDTLTL (681–689/A2) – HLA-B*15:17
MVYEDTLTL (681–689/A2) – HLA-B*35:08
FPSIRPIYL (1415–1423/B) – HLA-B*08:01
FPSIRPIYL (1415–1423/B) – HLA-B*07:04
FPSIRPIYL (1415–1423/B) – HLA-B*35:08
FIAAVERLW (1718–1726/A3) – HLA-B*57:01
FIAAVERLW (1718–1726/A3) – HLA-B*15:17
DQRIRWYLL (1956–1964/A3) – HLA-B*08:01
MASGHRDF (2046–2054/C1) – HLA-B*15:17
RYYLGAVEL (23–31/A1) – HLA-C*07:02
VYDTVVITL (99–107/A1) – HLA-C*07:02
VYDTVVITL (99–107/A1) – HLA-C*04:01
IFLEGHTFL (188–296/A1) – HLA-C*07:02
YFIAAVERL (1717–1721/A3) – HLA-C*07:02
YRGELNEHL (1767–1767/A3) – HLA-C*07:01
YRGELNEHL (1767–1767/A3) – HLA-C*07:02
YRGELNEHL (1767–1767/A3) – HLA-C*06:02
YRFHAINGY (1935–1946/A3) – HLA-C*07:01
YRFHAINGY (1935–1946/A3) – HLA-C*07:02
YRFHAINGY (1935–1946/A3) – HLA-C*06:02
0.17101 0.17101
0.20767 0.20767 0.20767
0.22980
0.17603
0.17484
0.21540
0.19617
0.17101
0.17101
0.23034 0.23034
0.23034
0.23034
0.22372
0.22372
0.40003 0.40003
0.19382
0.15081
0.26032
0.26032
0.26176
0.27427
0.19826 0.19826
0.19826
0.19826
0.24827 0.24827
0.24827
0.24827
R2228X
I22I
R1960X
0.40
0.35
0.30
0.25
0.20
HLA-A
R1960X
R2228X
0 0 0
1
1 0
0
I22I
HLA-B
R1960X
R2228X
4 2 2
1
0 1
0
I22I
HLA-C
R1960X
R2228X
0 0 0
2
1 0
3
I22I

Supplementary Figure 14. MHCII peptide presentation analysis.

(A) Total number of FVIII-derived peptides identified for HLA-DP, HLA-DQ, and HLA-DR alleles.

(B) Distribution of FVIII peptides across individual MHCII alleles.

(C) Predicted immunogenicity scores of peptides restricted to HLA-DP, DQ, and DR, with HLA-DP showing significantly higher values. Unpaired t-test significance: ***p<0.001.

(D) Immunogenicity of peptides stratified by FVIII domains (A1, A2, A3, C1). Representative peptide sequences with positions, domains, and scores are listed on the right. Bar graphs (far right) depict the proportion of top 10 peptides assigned to FVIII domains across the three patients (R1960X, R2228X, I22I). One-way ANOVA significance:*:p<0.1.

(E) Predicted cleavage probability of FVIII derived peptides by domains. Representative sequences with cleavage scores are listed on the right. Bar graphs (far right) show distribution of top 10 peptides across FVIII domains for the three patients.

(F) Predicted peptide loss associated with patient mutations. Venn diagram depicting in silico–predicted FVIII peptides absent due to the premature stop codons R1960X, R2228X, or I22I, with representative sequences listed.

(G) Venn diagram depicting overlap of high-immunogenic peptides among HLA-DP, HLA-DQ, and HLA-DR alleles. Shared and unique peptides are indicated below.

(H) Heatmaps of predicted peptide binding probability across HLA-DRB1, HLA-DRB345, HLA-DQA1/DQB1, and HLA-DPA1/DPB1 alleles aligned to patient mutations. Right panel: Venn diagrams depicting allele-specific overlap of presented peptides across three patients.

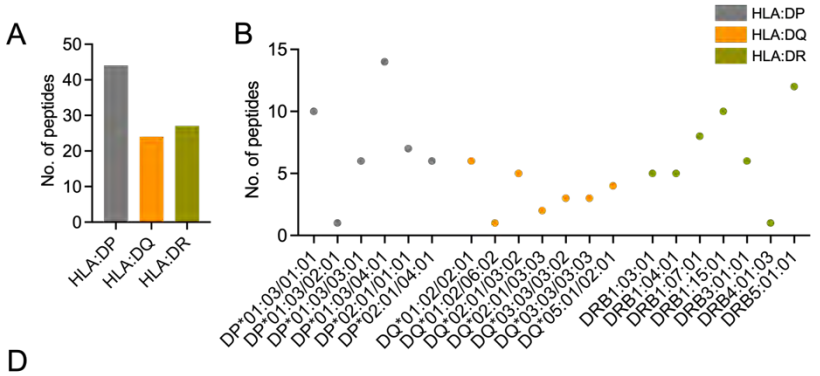

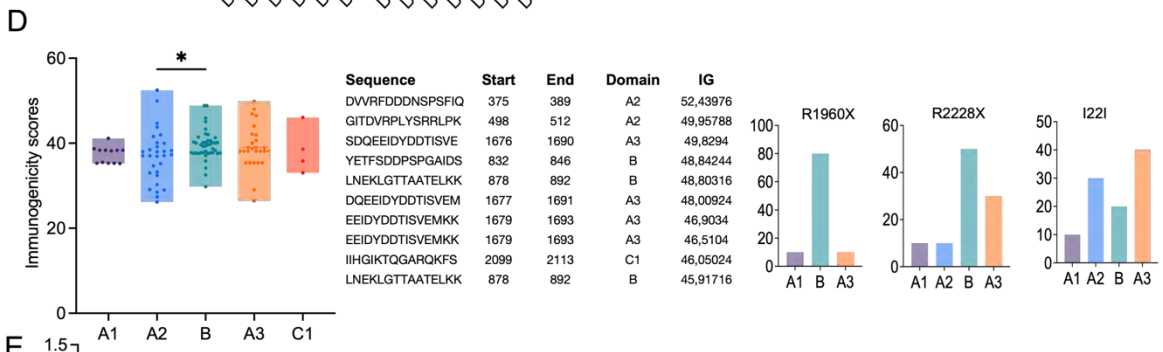

Sequence	Start	End	Domain	IG
DVVRFDDDNSPSFIQ	375	389	A2	52,43976
GITDVRPLYSRRLPK	498	512	A2	49,95788
SDQEEIDYDDTISVE	1676	1690	A3	49,8294
YETFSDDPSPGAIDS	832	846	B	48,84244
LNEKLGTTAATELKK	878	892	B	48,80316
DQEEIDYDDTISVEM	1677	1691	A3	48,00924
EEIDYDDTISVEMKK	1679	1693	A3	46,9034
EEIDYDDTISVEMKK	1679	1693	A3	46,5104
IIHGIKTQGARQKFS	2099	2113	C1	46,05024
LNEKLGTTAATELKK	878	892	B	45,91716

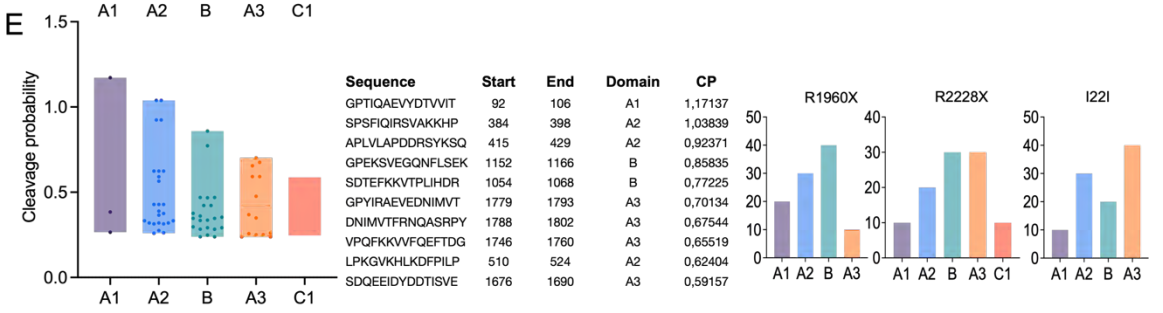

Sequence	Start	End	Domain	CP
GPTIQAEVYDTVVIT	92	106	A1	1,17137
SPSFIQIRSVAKKHP	384	398	A2	1,03839
APLVLAPDDRSYKSQ	415	429	A2	0,92371
GPEKSVEGQNFLSEK	1152	1166	B	0,85835
SDTEFKKVTPLIHDR	1054	1068	B	0,77225
GPYIRAEVEDNIMVT	1779	1793	A3	0,70134
DNIMVTFRNQASRPY	1788	1802	A3	0,67544
VPQFKKVVFQEFTDG	1746	1760	A3	0,65519
LPKGVKHLKDFPILP	510	524	A2	0,62404
SDQEEIDYDDTISVE	1676	1690	A3	0,59157

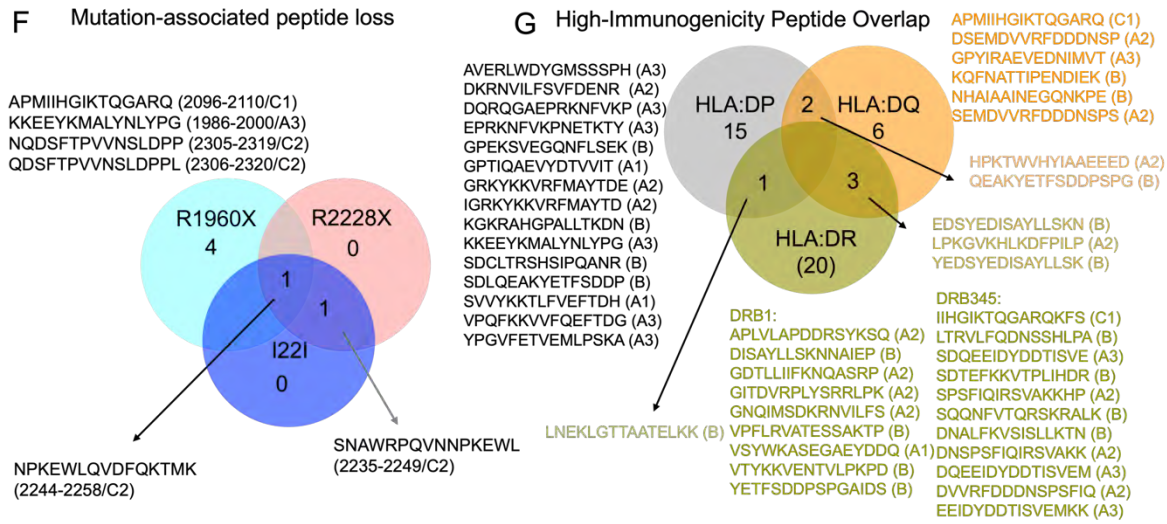

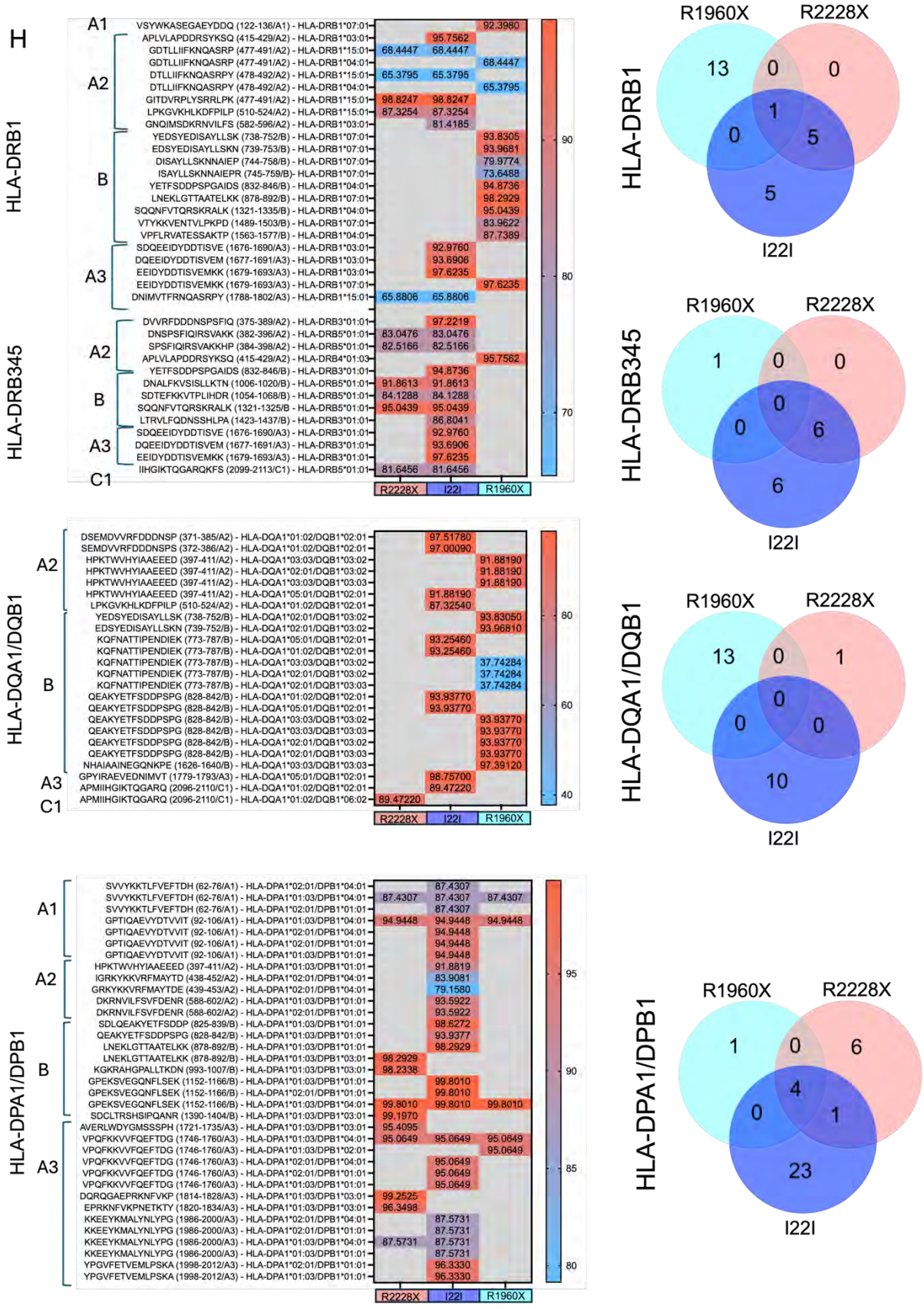
H
HLA-DRB1
HLA-DRB345
HLA-DQA1/DQB1
HLA-DPA1/DPB1
R2228X
I22I
R1960X
R1960X R2228X
13 0 0 1 0 5 5
I22I
R1960X R2228X
1 0 0 0 0 6 6
I22I
R1960X R2228X
13 0 1 0 0 0 10
I22I
R1960X R2228X
1 0 6 4 0 1 23
I22I

TABLE S1

REAGENT OR RESOURCE	SOURCE	IDENTIFIER
Antibodies		
Actin Smooth Muscle	ThermoFisher	Cat#MA5-11547; RRID: AB_11151920
Alpha-Fetoprotein	R&D Systems	Cat#MAB1368; RRID: AB_357658
Capture SelectTM	Thermo Fisher	Cat#7102862100
CD 144 Micro Bead Kit	Miltenyi Biotec	Cat#130-097-857;RRID: AB_2267145
CD 34 Micro Bead Kit	Miltenyi Biotec	Cat#130-046-702; RRID: AB_2848167
CD144	Santa Cruz	Cat#sc-9989; RRID: AB_2077957
CD144	BD Pharmingen	Cat#560874; RRID: AB_1645487
CD184	Miltenyi Biotec	Cat#130-117-690; RRID: AB_2728021
CD309(VEGFR2/KDR)	R&D Systems	Cat#FAB357P; RRID: AB_357165
CD31	Santa Cruz	Cat#sc-1506; RRID: AB_2161037
CD34	Miltenyi Biotec	Cat#130-113-178; RRID: AB_2726005
CD73	Miltenyi Biotec	Cat#130-123-802; RRID: AB_2889623
COPII (Sec31A)	Cell Signalling	Cat#13466; RRID: AB_2798228
GMA012	Green Mountain Antibodies	Cat#GMA012
GRP78 BiP	Abcam	Cat#ab21685; RRID: AB_2119834
LYVE1	ReliaTech	Cat#102-PA50
MHC-I PerCP-Vio700	Miltenyi Biotec	Cat#130-101-453; RRID:AB_2652093
MHC-II Clone WR18	Invitrogen	Cat#MA180680; RRID: AB_931650
Nanog	PeproTech	Cat#500-P236; RRID: AB_2929970
Oct4	abcam	Cat#ab19857; RRID: AB_445175
PDI (C81H6)	Cell Signalling	Cat#3501; RRID: AB_2156433
PROX-1	Abcam	Cat#ab101851; RRID: AB_10712211
SAF8C (affinity purified)	Affinity Biologicals	Cat#SAF8C-AP
SAF8C Peroxidase conjugated	Coachrom Diagnostica	Cat#SAF8C-HRP
SEL1L	antibodies-online	Cat#ABIN6132642
SSEA-4	Stemcell Technologies	Cat#60062; RRID: AB_2721031
ß-Tubulin	Stemcell Technologies	Cat#60100
STAB2	Abcam	Cat#ab121893; RRID: AB_11132688
Streptavidin Alexa 488	ThermoFisher	Cat#S32354; RRID: AB_2315383
Tra-1-60	Millipore	Cat#MAB4360; RRID: AB_2119183
VE-Cadherin	Santa Cruz	Cat#sc-9989; RRID: AB_2077957
vWF	Dako	Cat#A0082; RRID: AB_2315602
Chemicals, peptides, and recombinant proteins		
8-Br-cAMP	Biolog Life Science institute	BLG-B007-500
Accutase	Capricorn	ACC-1B
B27+Vit A	Thermofischer Scientific	17504-044
bFGF	PeproTech	100-18C-100
BMP4	PeproTech	120-05ET-10
BSA	Sigma	A1595
CHIR 99021	Biogems	2520691

DMEM F12/Glutamax	Thermofischer Scientific	31331093
ECGM-MV2	PromoCell	22121
EDTA	Sigma	E5134
ELISA substrate	Sigma Aldrich	11582950001
Fibronectin	Roche	10838039001
Forskolin	Stemcell	72114
Glycine	Geyer GmbH & Co. KG	3790.2
Growth factor reduced Matrigel	Corning	356230
IFN-γ	PeproTech	300-02-100
IL-1β	PeproTech	200-01B-10
IL-3	PeproTech	200-03-10
IL-6	PeproTech	200-06-20
L-685 458	Sigma	L1790
LDL-DyLightTM 550	Abcam	ab133127
Matrigel hESC-Quali mouse	Corning	354277
mTesR complete kit	Stemcell	85850
N2	Thermofischer Scientific	17502-048
NP40	Sigma Aldrich	R0278
Parafolmaldehyde	Sigma Aldrich	P6148
Penicillin-Streptomycin	Thermofischer Scientific	15070063
Protease inhibitor	Roche	4693159001
PureLink RNA Mini Kit	Invitrogen	12183018A
Purified Streptavidin	BioLegend	280302
ReadyProbesTM Streptavidi/Biotin blocking solution	ThermoFisher	R37628
Saponin	Fisher Scientific	15460297
SB-431542	BioVision	AOB 6359-1
Stempro 34 Kit	Thermofischer Scientific	10639011
TNF-α	PeproTech	300-01A-50
VEGF-A	PeproTech	100-20
VEGF-C	PeproTech	100-20-CD-100
Y-27632	Stemcell	2304
Critical commercial assays		
AgPath-ID-One step-RT-PCR Kit	Applied Biosystems	4387424
CaptureM™ IP & Co-IP kit	Takara	635721
Experimental models: Cell lines		
pHDLEC	Promocell	C-14021
pHUAEC	Promocell	C-14013
pHCMEC	Promocell	C-14029
pHUVEC	Promocell	C-14010
pLSEC	Neuromics	HEC11
Oligonucleotides and Primers		
AY-Actin F	Eurofins Genomics	ACC TTC TAC AAT GAG CTG CG
AY-Actin R	Eurofins Genomics	CCT GGA TAG CAA CGT ACA TGG
Probe-ACT	Eurofins Genomics	ACC TGG GTC ATC TTC TCG CGG TTG
PROX-1-F	Eurofins Genomics	GCC AGA TTT GCA GTC AAT GG
PROX-1-R	Eurofins Genomics	ATG ATG ACG TCG CCA AAG C
PROX-1-FAM	Eurofins Genomics	TTT CCA CAC CGC CAA C
PDPN-F	Eurofins Genomics	CAG GTG CCG AAG ATG ATG TG
PDPN-R	Eurofins Genomics	TGT TGC CAC CAG AGT TGT CA
PDPN-FAM	Eurofins Genomics	TGA CTC CAG GAA CCA G
LYVE-1 F	Eurofins Genomics	CTG GGT TGG AGA TGG ATT CG
LYVE-1 R	Eurofins Genomics	TCA GGA CAC CCA CCC CAT TT
LYVE1-FAM	Eurofins Genomics	TAG CCC AAA CCC CAA GTG

VEGFR3-F	Eurofins Genomics	CCT TGC CCG GGA CAT CTA
VEGFR3-R	Eurofins Genomics	TTG TCG AAG ATG CTT TCA GGG
VEGFR3-FAM	Eurofins Genomics	AGA CCC CGA CTA CGT CCG CAA GG
STAB2	Thermofischer Scientific	Hs00213948_m1
FCGR2B	Thermofischer Scientific	Hs00269610_m1
F8	Thermofischer Scientific	Hs00252034_m1
COUP-TFII	Thermofischer Scientific	Hs00819360_m1 I
VEGFR2	Thermofischer Scientific	Hs00911700_m1
NT5E	Thermofischer Scientific	Hs0015968_m1
Eph-B2	Thermofischer Scientific	Hs00187950_m1
vWF Ex38-39	Thermofischer Scientific	Hs01109449_m1
CD31	Thermofischer Scientific	Hs01065279_m1
CD34	Thermofischer Scientific	Hs02576480_m1
CD144 Ex3-4	Thermofischer Scientific	Hs00901465_m1
NANOG	Thermofischer Scientific	Hs02387400_g1
SOX2	Thermofischer Scientific	Hs04234836_s1
Brachyury	Thermofischer Scientific	Hs00610080_m1
Software and algorithms		
FlowJo	Tree Star	Version 10.9
GraphPad Prism	GraphPad Software	Version 10.4.1
Others		
0.45 µM filter	Berrytec	110597
LS columns	Miltenyi Biotec	130-042-401
MaxiSorp C8x12 (ELISA Plates)	VWR	735-0006
MicroAmp Optical 8-Cap Strip	Applied Biosystems	4323032
MicroAmp Optical 8-tube Strip (0.2mL)	Applied Biosystems	4316567
Vivaspin 6, MWCO: 50K	Sartorius	ST-2638
Mini Protean 7.5% MP TGX Gel	Biorad	4561024

Table S2: Quantitation for FVIII peptides detected in healthy. Green: High confidence peptides. M: measurement.

Peptide	First Position	Last Position	Healthy M1 Total area	Healthy M2 Total area
PYNIYPHGITDVRPLYSR	491	508		
DFPILPGEIFK	519	529	8,8E+05	
NVILFSVFDENR	591	602	4,5E+05	
SVEGQNFLSEK	1156	1166		
LWDYGMSSSPHVLR	1725	1738		
GELNEHLGLLGPYIR	1769	1783		2,0E+06
VDLLAPMIIHGIK	2092	2104		2,2E+05
HNIFNPPIIAR	2156	2166		
SNAWRPQVNNPK	2235	2246		1,7E+05
IHPQSWVHQIALR	2327	2339	7,0E+05	

Table S3: Quantification for Protein Disulfide Isomerase (PDI), an endoplasmic reticulum (ER) marker, and COPII as a marker for the ER-Golgi intermediate compartment (ERGIC) to localize FVIII in iLSEC

FVIII & PDI																				
Number of families	1																			
Number of comparisons per family	3																			
Alpha	0,05																			
																Cm1	I22I	R1960X	R2228X	
Dunnett's multiple comparisons test	Mean Diff.	95,00% CI of diff.	Below threshold?	Summary	Adjusted P	A-?								Number of values		59	65	57	65	
Cm1 vs. I22I	0,2195	0,1481 to 0,2908	Yes	****	<0,0001	B	I22I													
Cm1 vs. R1960X	0,07226	-0,001458 to 0,1460	No	ns	0,0561	C	R1960X							Minimum		0,2896	0,2086	0,1129	0,1885	
Cm1 vs. R2228X	0,05809	-0,01329 to 0,1295	No	ns	0,1376	D	R2228X							Maximum		0,925	0,8235	0,8717	0,8779	
														Range		0,6354	0,615	0,7589	0,6894	
Test details	Mean 1	Mean 2	Mean Diff.	SE of diff.	n1	n2		q	DF											
Cm1 vs. I22I	0,6617	0,4422	0,2195	0,03022	59		65	7,261	242					Mean		0,6617	0,4422	0,5894	0,6036	
Cm1 vs. R1960X	0,6617	0,5894	0,07226	0,03122	59		57	2,315	242					Std. Deviation		0,1503	0,1628	0,1932	0,1649	
Cm1 vs. R2228X	0,6617	0,6036	0,05809	0,03022	59		65	1,922	242					Std. Error of Mean		0,01957	0,02019	0,02559	0,02045	
FVIII & BiP																				
Number of families	1																			
Number of comparisons per family	3																			
Alpha	0,05																			
																Cm1	I22I	R1960X	R2228X	
Dunnett's multiple comparisons test	Mean Diff.	95,00% CI of diff.	Below threshold?	Summary	Adjusted P	A-?								Number of values		45	57	38	61	
Cm1 vs. I22I	0,2882	0,1892 to 0,3872	Yes	****	<0,0001	B	I22I													
Cm1 vs. R1960X	0,0421	-0,06727 to 0,1515	No	ns	0,6814	C	R1960X							Minimum		0,05804	0,00255	0,05121	0,03188	
Cm1 vs. R2228X	0,1884	0,09080 to 0,2859	Yes	****	<0,0001	D	R2228X							Maximum		0,8657	0,6929	0,9326	0,7666	
														Range		0,8076	0,6904	0,8814	0,7348	
Test details	Mean 1	Mean 2	Mean Diff.	SE of diff.	n1	n2		q	DF											
Cm1 vs. I22I	0,5545	0,2663	0,2882	0,04192	45		57	6,875	197					Mean		0,5545	0,2663	0,5124	0,3661	
Cm1 vs. R1960X	0,5545	0,5124	0,0421	0,04631	45		38	0,9091	197					Std. Deviation		0,2576	0,1906	0,2237	0,178	
Cm1 vs. R2228X	0,5545	0,3661	0,1884	0,04131	45		61	4,56	197					Std. Error of Mean		0,03839	0,02524	0,03629	0,02279	
FVIII & SEL1L																				
Number of families	1																			
Number of comparisons per family	3																			
Alpha	0,05																			
																Cm1	I22I	R1960X	R2228X	
Dunnett's multiple comparisons test	Mean Diff.	95,00% CI of diff.	Below threshold?	Summary	Adjusted P	A-?								Number of values		31	37	52	35	
Cm1 vs. I22I	0,05615	-0,05548 to 0,1678	No	ns	0,48	B	I22I													
Cm1 vs. R1960X	-0,1093	-0,2133 to -0,005241	Yes	*	0,0371	C	R1960X							Minimum		0,01433	0,00493	0,00526	0,00917	
Cm1 vs. R2228X	-0,04814	-0,1612 to 0,06493	No	ns	0,6047	D	R2228X							Maximum		0,6443	0,6967	0,8005	0,6979	
														Range		0,6299	0,6917	0,7952	0,6888	
Test details	Mean 1	Mean 2	Mean Diff.	SE of diff.	n1	n2		q	DF											
Cm1 vs. I22I	0,2719	0,2157	0,05615	0,04732	31		37	1,187	151					Mean		0,2719	0,2157	0,3812	0,32	
Cm1 vs. R1960X	0,2719	0,3812	-0,1093	0,0441	31		52	2,478	151					Std. Deviation		0,1791	0,1638	0,2186	0,1983	
Cm1 vs. R2228X	0,2719	0,32	-0,04814	0,04793	31		35	1,004	151					Std. Error of Mean		0,03217	0,02693	0,03032	0,03351	

Table S4: HLA genotypes of the three analyzed HA patients (R2228X, R1960X with inhibitor, and I22I) including class I (HLA-A, B, C) and class II (HLA-DR, DQ, DP) alleles.

	R2228X:	R1960X (Inhibitor):	I22I:
DRB1	HLA-DRB1*15:01	HLA-DRB1*04:01 HLA-DRB1*07:01	HLA-DRB1*03:01 HLA-DRB1*15:01
DRB345	HLA-DRB5*01:01	HLA-DRB4*01:03	HLA-DRB3*01:01 HLA-DRB5*01:01
DQA1/DQB1	HLA-DQA1*01:02/DQB1*06:02	HLA-DQA1*02:01/DQB1*03:03 HLA-DQA1*02:01/DQB1*03:02 HLA-DQA1*03:03/DQB1*03:03 HLA-DQA1*03:03/DQB1*03:02	HLA-DQA1*01:02/DQB1*02:01 HLA-DQA1*05:01/DQB1*02:01
DPA1/DPB1	HLA-DPA1*01:03/DPB1*03:01 HLA-DPA1*01:03/DPB1*04:01	HLA-DPA1*01:03/DPB1*02:01 HLA-DPA1*01:03/DPB1*04:01	HLA-DPA1*01:03/DPB1*01:01 HLA-DPA1*01:03/DPB1*04:01 HLA-DPA1*02:01/DPB1*01:01 HLA-DPA1*02:01/DPB1*04:01

	R2228X:	R1960X (Inhibitor):	I22I:
HLA-A	HLA-A*01:01 HLA-A*68:01	HLA-A*01:01 HLA-A*02:01	HLA-A*01:01 HLA-A*02:01
HLA-B	HLA-B*15:17 HLA-B*08:01	HLA-B*35:08 HLA-B*57:01	HLA-B*07:04 HLA-B*08:01
HLA-C	HLA-C*07:01	HLA-C*04:01 HLA-C*06:02	HLA-C*07:01 HLA-C*07:02